

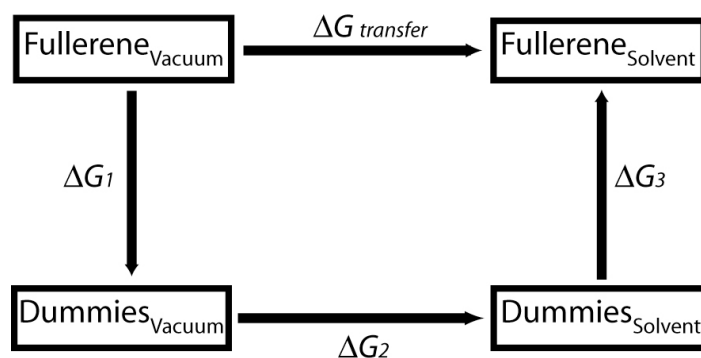
Parameterization of the fullerene coarse-grained model

We parameterized a coarse-grained fullerene consistent with the MARTINI coarse-grained force field for lipids¹ and proteins². In the MARTINI force field, approximately 4 non-hydrogen atoms are represented by a single interaction site. For fullerene, this means mapping approximately 4 carbons to 1 coarse-grained particle. An initial approximation for the location of the coarse-grained fullerene particles was obtained by placing 16 particles on a spherical surface with a diameter of 0.72 nm, and maximizing the inter-particle distances using a Monte Carlo method. The diameter of the sphere corresponds to the diameter of a real fullerene molecule^{3,4}. All the particles were then connected with an elastic network of bonds. The force constant for the bonds was 1250 kJ * mol⁻¹ * nm⁻².

For the non-bonded interactions of fullerene, we used as an initial approximation the same particle type used to represent benzene in the MARTINI force field¹. The parameters were then tuned to reproduce free energies of partitioning of fullerene between four organic solvents: benzene, cyclohexane, acetone and ethanol. The free energy of transferring fullerene from one solvent to the other was calculated using the thermodynamic integration formula:

$$\Delta G = \int_{\lambda=0}^{\lambda=1} \left\langle \frac{\partial H(\lambda)}{\partial \lambda} \right\rangle_{\lambda} d\lambda \quad (1)$$

and a thermodynamic cycle⁵:



For each solvent, a series of 29 simulations was performed with values of λ from 0 to 1. The λ values were not equally spaced and not identical in each simulation: smaller spacing was used close to the

steepest points in the $dG/d\lambda$ curve. The stochastic dynamics integrator was used, with an inverse friction coefficient of 1 ps. Each simulation was equilibrated for 20 ns and the production simulations were 400 ns long (formal simulation time). A soft-core potential was used for the non-bonded interactions to avoid the singularity in the potential when the interactions were turned off⁶. The soft-core parameter α , that controls the height of the potential around $r = 0$, was set to 1.3. The soft-core λ power was set to 1 and the range of the interaction (soft-core σ) was set to 0.47 nm.

Unbiased MD simulations: single fullerene and 16 fullerenes

In the unbiased simulations with one fullerene, the simulation box contained 72 lipids (either DOPC or DPPC) and 1593 water particles. In the simulations with 16 fullerenes, the simulation box contained 1152 DOPC and 12165 water particles. Parameters for the lipids and water were taken from the MARTINI force field¹. Non-bonded interactions were calculated using the standard procedure for the MARTINI force field: a 1.2 nm cutoff with switch function was applied for electrostatic and Lennard-Jones interactions; the distance to start switching Coulomb and van der Waals interaction was 0 and 0.9 nm, respectively. The neighbor list was updated every 10 steps and the relative dielectric constant for the medium was set to 15. Periodic boundary conditions were applied in all dimensions. The temperature for each group (lipid, water, fullerene) was kept at 300 K using the Berendsen temperature coupling algorithm with a time constant of 1 ps. Semi-isotropic pressure coupling was applied using the Berendsen algorithm, with a pressure of 1 bar independently in the plane of the membrane and perpendicular to the membrane, and a time constant of 5.0 ps. The integration time step was 40 fs (formal simulation time), and structures were saved every 100 ps for analysis. Based on comparison of diffusion constants in CG and atomistic simulations, the effective time sampled using our CG model is larger than the formal simulation time, and a similar scaling factor applies to all molecules in the simulated systems^{1, 7}. In the rest of the paper we use an effective time, instead of the formal simulation

time, and the conversion factor is a factor of four (*i.e.*, 1 ns formal simulation time corresponds to ca. 4 ns of real time).

Umbrella sampling simulations

All the simulation parameters and conditions were identical as for the unbiased simulations. A series of simulations was performed in which the fullerene was restrained at a given distance from the center of the bilayer using a harmonic potential. A force constant of $1000 \text{ kJ mol}^{-1} \text{ nm}^{-2}$ was used for the biasing potential in the direction of the bilayer normal, while no restraints were applied in the plane of the membrane. The distance between the fullerene and the center of the bilayer was increased from 0 to 4.5 nm with 0.1 nm increments. Each simulation was 800 ns long (effective time), for a total simulation time of 36.8 μs for each potential of mean force (PMF). Bilayers of two different sizes were used, containing 72 and 288 DOPC lipids, in order to verify the effect of the size of the bilayer on the free energy profile and on the deformations induced by fullerene. Further simulations were performed using a DPPC bilayer (72 lipids) at the temperature of 325 K (with identical computational parameters as for the DOPC simulations; total simulation time: 36.8 μs). These conditions are similar to those used by Qiao et al.⁸, and allow for a direct comparison between the force fields.

The PMF profile in DOPC shows a stabilization of approximately 110 kJ/mol when the fullerene is in the centre of the bilayer. The free energy profile is rather flat within 1.2 nm of the center of the bilayer, and the absolute free energy minimum is about 1 nm from the center. The highly polar and tightly packed lipid head group region represents a relatively small barrier that fullerene has to cross in order to enter the bilayer. This energy barrier is lower than 5 kJ/mol and is located around 2.9 nm from the center of the bilayer, corresponding to a close contact between fullerene and the choline group of the lipids. Despite its overall hydrophobic character, fullerene does not show a strong repulsion from the charged head group region of the bilayer. This can be explained by the number of dispersion interactions, which is higher in the denser parts of the bilayer (head group region).

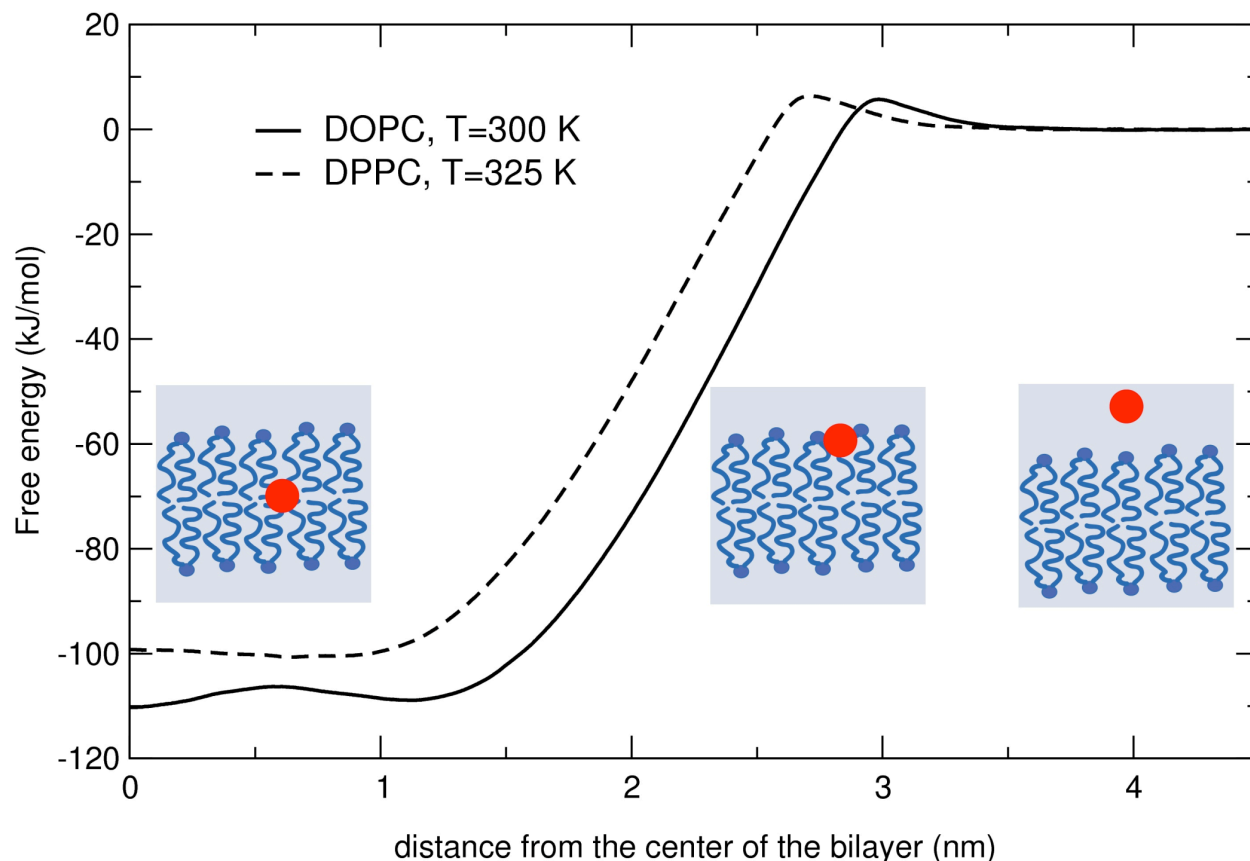


Figure 1S. The potential of mean force profile for fullerene as a function of the distance from the center of a lipid bilayer. A distance of zero represents the center of the bilayer. The free energy was set to zero in bulk water.

Comparison between atomistic and coarse-grained simulations

The PMF profile in DPPC is qualitatively similar to the one in DOPC. The total stabilization is about 98 kJ/mol when the fullerene is in the centre of the bilayer, and the free energy reaches a minimum around 0.9 nm from the center (~100 kJ/mol). Compared to the profile in DOPC, the energy maximum is closer to the bilayer centre (2.65 nm instead of 2.9 nm) and the energy barrier is about the same. Comparing to atomistic simulations by Qiao et al.⁸, the difference in energy between the minima is significant: atomistic simulations gave a total stabilization of approximately 35 ± 8 kJ/mol. On the other

hand, the position of the energy minimum, about 1 nm from the center of the membrane, is in excellent agreement.

Two unbiased MD simulations were performed for a single fullerene molecule in the presence of a DPPC bilayer, in order to compare the kinetics of spontaneous permeation. In both simulations, the time required for crossing the head group region was similar to the DOPC case (~500 ps on average in DOPC, 450 ps in DPPC). This is longer than observed in atomistic simulations (~70 and ~160 ps in reference ⁸), although on the same time scale. In conclusion, agreement with atomistic simulations is only qualitative, both for the kinetics and the thermodynamics of the processes investigated.

Two reasons can be indicated for the deviations from atomistic results: first, differences in the details of the force fields; second, insufficient sampling in atomistic simulations, due to prohibitively high computational cost. It is difficult to say which force field provides the most realistic estimate: while atomistic force fields are in general more accurate in reproducing experimental results, all-atom models of fullerene used in all previous studies (to the best of our knowledge) have not been validated against experimental solvation or partitioning data, which is the main determinant for partitioning in a membrane system. In particular, it is known that the GROMACS force field (used by Qiao et al.⁸) and GROMOS versions previous to 53A5/53A6 do not faithfully reproduce experimental free energies of solvation (nor partitioning between organic solvents) for common amino acid side chains^{9, 10}. Ideally, a realistic estimate of fullerene partitioning between water and lipid membranes could be obtained by parameterizing non-bonded interactions of fullerene based on partitioning between water and alkanes. Unfortunately such information is not available from the literature, to the best of our knowledge, due to extremely low solubility of fullerene in water (not accurately measurable).

Calculation of fullerene permeability

The solute was constrained at the chosen depths inside the bilayer and the constraint forces were calculated as a function of the simulation time. We used the force autocorrelation method for the calculation of the local time-dependent friction coefficient ($\xi(t)$):

$$\xi(t) = \frac{\langle \Delta F(z,t) \cdot \Delta F(z,0) \rangle}{RT} \quad (8)$$

where R is the universal gas constant, T is the absolute temperature and

$$\Delta F(z,t) = F(z,t) - \langle F(z) \rangle_t \quad (9)$$

is the time fluctuation in the instantaneous force on the constrained particle (in the direction of the constraint, z).

The static friction coefficient $\xi = \int_0^\infty \xi(t) dt$ is inversely proportional to the local diffusion coefficient ($D(z)$)¹¹⁻¹³:

$$D(z) = \frac{RT}{\xi} = \frac{(RT)^2}{\int_0^\infty \langle \Delta F(z,t) \cdot \Delta F(z,0) \rangle dt} \quad (10)$$

Diffusion coefficients calculated at the center of bilayer and in bulk water are consistent with results from unbiased simulations.

The permeability coefficient (P) of the solute is defined as the inverse of the overall membrane resistance (R) to fullerene permeation:

$$R = \int_{outside}^z \frac{\exp(\Delta G(z')/RT)}{D(z')} dz' = \frac{1}{P} \quad (11)$$

A series of constraint simulations were run with the distance between fullerene and the center of the bilayer constrained between 0 and 4.5 nm, with 0.1 nm spacing. Only the component of the distance normal to the bilayer (z axis) was constrained, while the solute was completely free to move in the x and y directions. The SHAKE algorithm was used¹⁴, with a relative tolerance of 10^{-5} . As for the umbrella sampling simulations, each constraint simulation was 800 ns long (effective time), for a total simulation time of 36.8 μ s.

Fullerene translocation from solid-like aggregate into water: thermodynamic integration

512 fullerene molecules were arranged on a regular grid (8 x 8 x 8 molecules) in a very compact, solid-like arrangement. This “solid” fullerene aggregate was equilibrated for 2 μs at constant temperature (300 K) and pressure (1 μs at 100 bar; 1 μs at 1 bar) in order to obtain the most stable possible arrangement. The free energy for transferring one fullerene from the solid-like aggregate to the gas phase was calculated using thermodynamic integration. The final structure of the equilibration run was used as a starting structure for the thermodynamic integration runs. The stochastic dynamics integrator was used, with an inverse friction coefficient of 1 ps. A series of 29 simulations was performed with values of λ from 0 to 1. Each simulation was equilibrated for 100 ns, while the length of the production runs was between 400 ns and 6.4 μs (effective time). Longer simulations were necessary in some cases to reduce the value of the error estimate. Error estimates on the free energy derivative were calculated by block averaging¹⁵. A soft-core potential was used for the non-bonded interactions to avoid the singularity in the potential when the interactions were turned off⁶. The same soft-core parameters were used as for the calculation of partitioning free energies (see above). The free energy of transfer of monomeric fullerene from the gas phase into bulk water was also calculated using thermodynamic integration, with a similar procedure and parameters. Production runs in this case were 1.6 μs long.

Calculation of the membrane properties as a function of fullerene concentration

The simulation boxes contained 1152 lipids and approximately 12200 water particles. All the simulation parameters were the same as described above, except for the pressure and temperature coupling. The Nose-Hoover thermostat and the Parrinello-Rahman barostat were used to generate the appropriate (NPT) thermodynamic ensemble.

Lateral diffusion coefficients of the lipids were calculated from the mean squared displacement (MSD) of the lipids as a function of time. Motion of each membrane leaflet relative to each other and to water was removed by subtracting the center of mass motion of each monolayer before calculating the MSD, as explained in ¹⁶. Diffusion coefficients were calculated using the model by Wohlert and Edholm¹⁶, considering two diffusion regimes with different time scales. The equation describing lipid diffusion is:

$$\langle r^2 \rangle = \frac{4D_1 t r_0^2}{r_0^2 + 4D_1 t} + 4D_2 t,$$

where D_1 is the diffusion coefficient at short time scales, D_2 is the diffusion coefficient at long time scale, t is time, $r_0^2 \equiv \frac{R^2}{2}$ and R is the radius of the circular area within which lipids diffuse on the short time scale.

The area compressibility modulus K_A was calculated from the fluctuations in the projected area of the membrane using the relation:

$$K_A = k_B T \frac{A}{N \langle (A - A_0)^2 \rangle}$$

where A is the area per lipid, k_B is the Boltzmann constant, T is the absolute temperature, N is the number of lipids in each leaflet and A_0 is the average area per lipid. The bending modulus was calculated from the undulation spectrum [see references ¹⁷ and ¹⁸]. According to a continuum model, the average squared amplitude of the undulations, $\langle u_{und}^2 \rangle$ is related to the bending modulus k_c through the wave vector q :

$$\langle u_{und}^2(q) \rangle = \frac{k_B T}{A} \left(\frac{1}{k_c q^4 + \gamma q^2} \right) \quad \text{for } q < q_0$$

where γ is the surface tension ($\gamma = 0$ in our simulations), $q_0 = 2\pi/h_0$ and h_0 is the average membrane thickness. This assumes the absence of a spontaneous curvature, which is justified for a symmetric bilayer, and is only valid at length scales significantly larger than the membrane thickness.

References

1. Marrink, S. J., Risselada, H. J., Yefimov, S., Tieleman, D. P. & de Vries, A. H. The MARTINI forcefield: coarse grained model for biomolecular simulations. *J. Phys. Chem. B* **111**, 7812-7824 (2007).
2. Monticelli, L. et al. The MARTINI coarse-grained force field: extension to proteins. *J. Chem. Theory Comput.* **in press**, (2008).
3. Sumpter, B. G. & Noid, D. W. The Onset of Instability in Nanostructures - the Role of Nonlinear Resonance. *J. Chem. Phys.* **102**, 6619-6622 (1995).
4. David, W. I. F. et al. Crystal structure and bonding of ordered C60. *Nature* **353**, 147-149 (1991).
5. Villa, A. & Mark, A. E. Calculation of the free energy of solvation for neutral analogs of amino acid side chains. *J. Comput. Chem.* **23**, 548-553 (2002).
6. Beutler, T. C., Mark, A. E., Vanschaik, R. C., Gerber, P. R. & Van Gunsteren, W. F. Avoiding Singularities and Numerical Instabilities in Free-Energy Calculations Based on Molecular Simulations. *Chem. Phys. Lett.* **222**, 529-539 (1994).
7. Marrink, S. J., de Vries, A. H. & Mark, A. E. Coarse grained model for semiquantitative lipid simulations. *J. Phys. Chem. B* **108**, 750-760 (2004).
8. Qiao, R., Roberts, A. P., Mount, A. S., Klaine, S. J. & Ke, P. C. Translocation of C60 and its derivatives across a lipid bilayer. *Nano Lett.* **7**, 614-619 (2007).
9. Maccallum, J. L. & Tieleman, D. P. Calculation of the water-cyclohexane transfer free energies of neutral amino acid side-chain analogs using the OPLS all-atom force field. *J. Comput. Chem.* **24**, 1930-1935 (2003).
10. Oostenbrink, C., Villa, A., Mark, A. E. & Van Gunsteren, W. F. A biomolecular force field based on the free enthalpy of hydration and solvation: The GROMOS force-field parameter sets 53A5 and 53A6. *J. Comput. Chem.* **25**, 1656-1676 (2004).
11. Kubo, R. The fluctuation-dissipation theorem. *Rep. Prog. Phys.* **29**, 255-284 (1966).
12. Kirkwood, J. G. The Statistical Mechanical Theory of Transport Processes I. General Theory. *J. Chem. Phys.* **14**, 180-201 (1946).
13. Marrink, S. J. & Berendsen, H. J. C. Permeation process of small molecules across lipid membranes studied by molecular dynamics simulations. *J. Phys. Chem.* **100**, 16729-16738 (1996).
14. Ryckaert, J. P., Ciccotti, G. & Berendsen, H. J. C. Numerical integration of Cartesian Equations of Motion of a System with Constraints - Molecular Dynamics of N-Alkanes. *J. Comput. Phys.* **23**, 327-341 (1977).

15. Allen, M. P. & Tildesley, D. J. *Computer simulation of liquids* (Oxford University Press, 1987).
16. Wohrlert, J. & Edholm, O. Dynamics in atomistic simulations of phospholipid membranes: Nuclear magnetic resonance relaxation rates and lateral diffusion. *J. Chem. Phys.* **125**, 204703-204710 (2006).
17. Lindahl, E. & Edholm, O. Mesoscopic undulations and thickness fluctuations in lipid bilayers from molecular dynamics simulations. *Biophys. J.* **79**, 426-433 (2000).
18. Marrink, S. J. & Mark, A. E. Effect of undulations on surface tension in simulated bilayers. *J. Phys. Chem. B* **105**, 6122-6127 (2001).